ELSEVIER

Materials Science and Engineering B74 (2000) 125–132

MATERIALS SCIENCE & ENGINEERING B

www.elsevier.com/locate/mseb

Characterization of quantum well structures using surface photovoltage spectroscopy

N. Ashkenasy *, M. Leibovitch, Y. Rosenwaks, Yoram Shapira

Department of Physical Electronics, Faculty of Engineering, Tel-Aviv University, Ramat-Aviv, 69978, Israel

Abstract

In this work a novel method to characterize quantum well (QW) structures and devices is presented. The method is based on the well-known surface photovoltage spectroscopy (SPS) and on numerical simulations. It is shown that the surface photovoltage is sensitive to the electron hole energy transition levels in the well layer as well as to features of other regions of the structure. The photovoltaic response as function of well width is numerically studied and is found to increase with decreasing well width. As a result of the spectra analysis growth parameters such as quantum well width and ternary layer composition (both of quantum well and cladding layers) are accurately determined. In addition, structure properties such as electric fields and effective carriers lifetime at the well are estimated. Finally it is shown that operating device parameters such the lasing wavelength may also be obtained. The results demonstrate the power of SPS as a characterization method for QW structures and devices in a contactless and non-destructive manner.

Keywords: Quantum well; Photovoltage; Device characterization

1. Introduction

The emerging growth techniques, such as molecular beam epitaxy (MBE) and metal organic chemical vapor deposition (MOCVD), have made it possible to grow solid films with thickness below the Bohr radius of the material [1]. In such thin structures, electrons and holes are confined to a very small volume in one or more dimensions and therefore exhibit quantum size effects. The electron and hole energy levels are quantized and the density of states (DOS) of the valence and conduction bands is changed [1]. Since the energy levels and the DOS control both the optical and the electrical properties of the structure, these properties are different in low dimensional structures (LDSs) with regard to the bulk material.

Another very important phenomenon which occurs in LDSs is increased exciton binding energy and oscillator strength for optical transitions [1,2]. Thus, excitons become stable at higher temperatures as compared to bulk material [3]. The properties of LDSs are of great interest for basic physics research. In addition, the ability to engineer these properties by means of growth parameters have led to development of new devices and figure of merit improvement of other devices, based on those LDSs.

The development of low dimensional structures and devices requires non-destructive and wafer-scale characterization methods, which can resolve the changes in the DOS and the induced electrical and optical properties. Those methods should be contactless and capable of in situ and/or ex situ characterization of the LDS. Determination of the electric potential distribution in the entire structure is of great importance (in order to evaluate and monitor the quantum confined Stark effect (QCSE) [2]). Common characterization techniques such as absorption/transmission, photoluminescence (PL), photoluminescence excitation (PLE) spectroscopy [3], and photoreflectance (PR) (for a review on this method and its applications see Refs. [4–6], are usually employed for such studies. Photoelectric techniques, namely photoconductivity (PC) and photovoltage (PV), have also been employed for LDS characterization [7–12].These techniques are very sensitive to the absorption of the exciting illumination. Thus, they are essentially as good as absorption/transmission experi-

* Corresponding author. Tel.: +972-3-6408015; fax: +972-3-6423508.

E-mail address: nurit@eng.tau.ac.il (N. Ashkenasy)

0921-5107/00/$ - see front matter
PII: S0921-5107(99)00547-4

ments for measuring the excitonic absorption peaks of quantum structures, without the need for etching. However, they do require forming a junction which includes the low dimensional region, a process which affects the electronic structure of the top layers via the top contact and adds to the complexity of the measurement. In the last few years, non-destructive measurement techniques which measure the PV spectra by means of capacitive [13–15] and magnetic [16] coupling have also been suggested but the scope of the obtained quantitative information is limited.

A different method for gauging the PV signal at surfaces and interfaces of semiconductor structures is surface photovoltage spectroscopy (SPS) [17]. This method monitors changes in the surface work function due to light illumination (i.e. the surface photovoltage (SPV)) using the well-known Kelvin probe method [18]. In this method the difference between the work function of a reference electrode and the semiconductor surface work function, which is also known as the contact potential difference (CPD), is measured by means of capacitive coupling.

The formation of an SPV requires both photo-generation and separation of charge carriers. Therefore, the obtained SPV spectrum contains information about both the optical and electrical properties of the structure. Bandgap energies and defect state characteristics can be monitored [17,19]. In addition, previous works have shown that Kelvin-probe-based measurements may lead to the determination of growth parameters, such as material composition [20] and doping [21,22]. In the past decade, the quantitative and qualitative analysis of buried interfaces has been extensively studied [21–25]. The ability to perform optical and electrical characterization of buried interfaces and multi-layer structures in a contactless and non-destructive manner has led to the use of SPS as a quality control tool, especially of solar cell devices [26–29]. It has also been applied to characterization of novel heterostructure bipolar transistors [30]. Further details on SPV phenomena and its applications are reviewed in Ref. [17]. These studies imply that SPS may be used for investigating LDSs and devices for both basic research and technology. To do that the PV response of such complex structures should be fully understood and its sensitivity to quantum effects should be utilized for device characterization.

This work describes a methodology for LDS characterization, using SPS combined with numerical simulations. In Section 2, the experimental set-up and numerical simulations are described. In Section 3, the SPV spectrum is shown to be sensitive to the quantum confined transition levels of GaAs/AlGaAs multi quantum well (MQW) structures. The PV response of single quantum well (QW) *p-i-n* structures is discussed in Section 4. These studies are applied in Section 5 for the estimation of carrier lifetimes at the well. In addition, the SPV spectrum is applied for quantitative characterization of growth and structure parameters of a graded-index-of-refraction-separate-confinement-heterojunction (GRINSCH) laser structure. The results are summarized in Section 6.

2. Experimental set-up

In order to perform the SPS measurement a light from a tungsten halogen is passed through a grating monochromator and a filter monochromator (Oriel, USA). A commercially available Kelvin probe (Besocke Delta Phi, Jülich, Germany) is used for the CPD measurement. The measurement rate is set so that a steady state is achieved at each wavelength prior to the CPD reading. All measurements presented in this work were performed at room temperature and in air atmosphere.

The transition levels in QW structures have been numerically studied by simulation. The simulation solves the Schrödinger equation using the envelope function approximation [3] with appropriate boundary conditions [31]. Effects of strain are also taken into account where needed. Another comprehensive, self-consistent simulation that simultaneously solves the continuity equation, Poisson equation and the Schrödinger equation when required [32–34] is used to obtain calculated SPV spectra and fit them to the experimental spectra.

3. Surface photovoltage spectra of multi quantum well structures

In this section the ability of SPS to monitor the transition levels of QW structures is discussed. A MQW structure was used to overcome the small absorption volume of a QW layer. The MQW sample consisted of 85 periods of GaAs (75 Å) and $Al_xGa_{1-x}As$ ($x=0.2$, 100 Å) between a bottom layer of a 0.5-μm thick $Al_xGa_{1-x}As$ ($x=0.3$) barrier followed by a 0.5-μm GaAs epilayer, and a top layer of a 0.5-μm thick $Al_xGa_{1-x}As$ ($x=0.3$). All layers were unintentionally doped, implying a nominal doping of about $p=1\times10^{15}$ cm^{-3} and $p=1\times10^{16}$ cm^{-3} for the GaAs and $Al_xGa_{1-x}As$ layers, respectively (the samples were grown by Dr M. Hanna, NREL, Golden, CO, USA).

Fig. 1 shows the SPV spectra of the MQW sample after etching in 1:8:500 H_2SO_4:H_2O_2:H_2O for 4 min (corresponding to the removal of $\sim$200 nm of the $Al_{0.3}Ga_{0.7}As$ top layer). For interpreting the spectrum, the following convention is used for slope change signs. The sign is positive if the illumination-induced change in electric field drives holes towards the surface, and vice versa [35]. The SPV spectrum of Fig. 1 has many

features: the slope change at 1.38 eV corresponds to the onset of band-to-band absorption in the GaAs epilayer (beginning at energies below the nominal bandgap due to the Franz-Keldysh effect [36]). The positive sign of the slope indicates that the energy bands are bent downwards toward the surface in the dark. The slope change around 1.78 eV corresponds to the onset of band-to-band absorption in the AlGaAs cap layer (the nominal bandgap being 1.79 eV). Again, the bands are bent downwards in the dark.

In the photon energy range of 1.43–1.75 eV, the SPV spectrum is expected to be governed by absorption in the MQW region. Indeed, the shape of the spectrum in this region resembles typical absorption spectra of MQW structures. Since the slope is negative at energies around 1.43 eV, the bands are bent upwards and the excitonic absorption peaks should be observed as minima in the spectra as can be seen in the figure. Note that the total SPV changes sign (from positive to negative) in this regime. Hence, the mimina must be due to photovoltaic activity in the MQW region itself. They cannot be simply due to modulation of the light intensity falling on the GaAs bottom layers by the MQW transmittance, as was suggested by former works on PV effects of QW structures [37,38]. Two minima are observed, at 1.48 and 1.61 eV. The SPV spectrum in the MQW absorption energy range has not changed at all (other than undergoing a uniform shift) after the etch. Hence, we have ascertained that the signal in the MQW absorption range is not due to surface effects.

The observed excitonic peaks agree well with the energy values of the calculated 1HH-1E and 2HH-2E neglecting electric field effects [1]. (The notation mH(L)H-nE is assigned to the transition between the mth heavy (light) hole level to the nth electron level). Moreover, the 1HH-1E transition energy is consistent with that found using room temperature PL (not shown). The higher transition was not detected by the PL measurement. A rigorous numerical analysis of the SPV spectrum has also been performed. The band

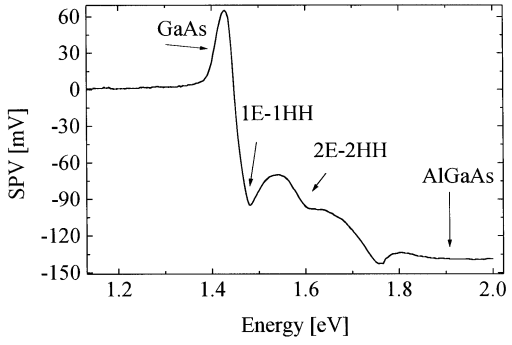

Fig. 1. SPV spectra of the MQW sample after etching for 4 min (arrows denote minima corresponding to heavy-hole-electron transition peaks).

diagram of the structure has been obtained by using the nominal material composition and doping assuming an external surface charge density of $\sim 6 \times 10^{-8}$ C cm^{-2} [39]. The diagram qualitatively confirms our experimental findings regarding the band bending lineup in the sample. Moreover, it shows that the electric field anywhere within the MQW region is small enough so that the QCSE is negligible, thereby explaining the good agreement between our measurements and the simple calculation mentioned above.

Since SPS resolves all 'symmetry-allowed' heavy-hole-electron transition in the QWs, it provides an easy means of monitoring any deviation from desired parameters during growth. This is because higher transitions are much more sensitive to fluctuations in QW parameters (e.g. well width and barrier composition), thus leading to a quantitative characterization of both growth and operating device parameters. Two examples for such quantitative characterization will be given in Section 4.

4. Photovoltaic behavior of quantum well structures

Since the photovoltaic behavior of semiconductor structures is governed by their optical and electronic properties, it is strongly affected by the presence of a QW in the structure. The magnitude of the PV is determined by the electron and hole spatial distribution throughout the entire structure. Thus, the presence of QW layers can affect the PV value through several different mechanisms. (i) A shift in the well effective bandgap, E_W. This may affect the PV in a similar fashion to the effect of the semiconductor bandgap on a solar cell open circuit voltage, V_{OC} [40]. (ii) An increase in oscillator strength, f_W, which determines the magnitude of the absorption coefficient, α_W, and thus the generation rate in the well [1]. (iii) A decrease in QW carrier lifetime, τ_W, due to a larger overlap between the electron and hole wave functions and a reduced exciton Bohr radius [3]. (iv) The width of the QW layer, w, which affects the excess carrier concentration because it controls the well generation/recombination, (G/R) volume.

In this section the SPS technique is used to determine the PV behavior of single QW p-i-n structures. Using this technique the PV response is measured under open circuit conditions, in a non-destructive contactless manner, making it possible to monitor the structure open circuit behavior at the early process stages of device formation.

The PV modification due to quantum effects was studied using single QW p-i-n diode structures which were grown by metal organic vapor phase epitaxy (MOVPE) on a heavily doped GaAs(001) n^+ substrate. The i layer consisted of a GaAs well with well widths of

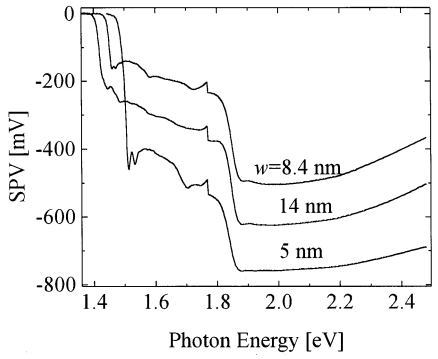

Fig. 2. Experimental SPV spectra of QW *p-i-n* structures with different well widths as indicated.

$w = 5$, 8.4, and 14 nm sandwiched between 150-nm thick $Al_{0.34}Ga_{0.64}As$ layers. The cladding consisted of 150-nm thick $Al_{0.34}Ga_{0.64}As$ layers with $n = 2 \times 10^{17}$ cm^{-3} at the bottom and $p = 9 \times 10^{17}$ cm^{-3} at the top of the structure. This was followed by a 20-nm thick GaAs layer with $p = 2 \times 10^{18}$ cm^{-3}. Further details are given in Ref. [41].

The SPV spectra of the three samples are shown in Fig. 2. The large probe size (2.5 mm in diameter) and the repeatability of these spectra over different areas on the sample indicate that these spectra manifest the average PV behavior for the measured samples. The overall negative PV response is due to the reduction of the built-in voltage at the junction under illumination.

Two main regions are observed in the spectrum. Absorption in the GaAs QW governs the low energy region (below ~ 1.8 eV). It resembles the absorption spectrum of QW structures, where the spectral minima lie at the exciton transition energies. This is similar to the PV behavior shown in Fig. 1 for the MQW structure. The second region of the spectrum appears as a second drastic decrease in the PV at ~ 1.8 eV. This decrease is due to absorption in the $Al_{0.34}Ga_{0.66}As$ layers of the structure. The feature at 1.7 eV is an experimental artifact due to change of optical filters.

Comparing the magnitude of the PV response for the three different samples shows that the differences are constant for the entire spectral range (except for the energies of the excitonic peaks). The 5- and 8.4-nm thick well samples have the largest and smallest responses, respectively. This is not consistent with V_{OC} values measured for similar structures, which show an increase of V_{OC} with decreasing well width [42,43]. The possible reasons for this inconsistency are discussed in Section 5.

The quantum PV effect has been calculated numerically. After establishing the separate contribution of each of the well parameters to the PV response, the general dependence of the PV on w was evaluated by estimating the dependence of each parameter on w and inserting the values into the numerical simulation. The blue shift in the absorption edge has been directly estimated from the experimental results. E_W was considered as the first minimum of the spectrum for each corresponding w. Typical values for τ_W were chosen according to Ref. [3]. The value of f_W for the 5-nm thick well was adjusted to fit its experimental PV response, and for the following calculations its theoretical dependence on w was taken into account [44,45]. The values of τ_W and f_W are accurate within the accuracy of τ_5. (This is since the excess carrier concentration depends on the product $G \cdot \tau$ [39].)

The results of these simulations are presented in Table 1 in the column labeled PV_1, together with the values of E_W, τ_{Wi} and f_W used in the calculations. The results show that the PV response of single QW *p-i-n* structures should increase with decreasing well width as shown experimentally for V_{OC} of similar structures [41,42]. Thus, the changes in f_W and E_W with decreasing w, which tends to increase the PV, are more dominant than the change of τ_W, which tends to decrease the PV, in determining the PV response. This also explains the super-linear change in V_{OC} as a function of the well bandgap [41,42]. Thus, when all the quantum effects are taken into account, the PV response is larger than in the case when only the blue shift effect is taken into account.

Table 1
Experimental and simulated PV[a]

w (nm)	PV (mV)	E_W (eV)	f_W[b] (arb. units)	τ_{Wi}[c] (ns)	PV_1 (mV)	τ_{Wc} (ns)
	Experimental				Calculated	Estimated
5	−424	1.514	0.02	0.2	−418	0.2
8.4	−192	1.461	0.014	0.3	−399	0.004
14	−306	1.447	0.011	0.6	−393	0.1

[a] Response at a photon energy of 1.6 eV together with the values used in the simulations (E_W, f_W, τ_{Wi}). Explanations are in the text.
[b] After Refs. [44] and [45], normalized to fit the PV of the 5-nm thick well structure.
[c] After Ref. [3].

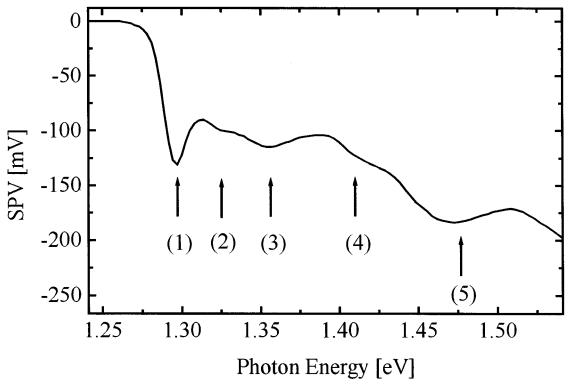

Fig. 3. The SPV spectrum at 700 nW cm^2 for photon energies below 1.55 eV. (Transition energies are indicated by arrows.)

5. Extraction of structural and device parameters

The main objective of this section is to develop a simple method that will make it possible to extract structural and device properties using SPS measurements and analysis.

5.1. Estimation of effective carrier lifetime in the well

Having established the quantum effects on the PV response of QW *p-i-n* structures in Section 4, we focus on the analysis of the experimental spectra. Comparing the experimental data in Fig. 2 and the results of the calculations shows that at least one of the samples does not respond as expected by the calculations. The PV of the 14-nm thick sample is expected to be smaller than that of the 8.4-nm thick sample, which is evidently not the case. Such behavior may originate in growth quality variations and not in quantum effects.

Two growth quality factors, namely the surface potential, V_S, and τ_W, may influence the SPV. As mentioned in the introduction, the Kelvin probe method is very sensitive to changes in V_S [17]. Since the top layer of the entire measured structure is a p^+-GaAs, the change in the SPV is expected to be small because of the high doping concentration. In addition, it should be positive for photon energies higher than the bulk GaAs absorption edge since in a *p*-type semiconductor the bands bend down toward the surface in the dark. Such behavior is not observed for any of the samples and thus the V_S effect on the PV response of the three samples is believed to be small. Therefore, the changes in the PV response should originate in τ_W. Our numerical simulations indicate that the recombination at the well is the dominant recombination mechanism for excess carriers throughout the structure. Fluctuations in the quality of the GaAs well layer would result in changes in τ_W (if the non-radiative processes dominate the recombination) and thus affect the entire PV spectrum. Therefore, comparing the dependence of the PV response on τ_W, which were found by the numerical calculation, with the experimental spectrum would result in estimation of the carrier effective lifetime at the well, τ_{Wc}, for the studied structures. These values of τ_{Wc} are presented in Table 1. Again, it should be noted that the accuracy of these values depends on the accuracy in evaluating τ_5. Nonetheless, the ratio between τ_{Wc} of the different samples should be relatively close to the real ratio. These results indeed show that the non-radiative processes govern the excess carrier recombination at room temperature. Based on these results, it seems that typical values of τ_W lie within the range of several hundreds of ps and are weakly dependent on *w*. This would make the increase in the PV response with decreasing well width even more pronounced. Yet, fluctuations in growth quality may result in much smaller τ_W, as was observed for one of the studied samples. These fluctuations in τ_W can be monitored by SPS in a contactless non-destructive manner, leading to quality control of the structure in early stages of device preparation. Such measurements may also lead to a rough estimation of V_{OC} of the final device.

5.2. GRINSCH laser structure growth and device parameters

In the introduction we have emphasized that the energy levels and optical transitions at LDSs are controlled by the layer width, alloy composition, number of quantum confining layers, distance between the layers, as well as the complete device band line-up. In particular, determining the electric potential distribution in the entire structure is a crucial step for LDS characterization. This affects the DOS through the quantum QCSE, which in turn affects device performance [46]. Transition energy positions and amplitudes can be monitored as was demonstrated in the previous sections. In this section a GRINSCH laser structure is characterized by means of growth parameters and lasing wavelength.

The GRINSCH *p-i-n* diode laser used in this work was grown by MBE on a GaAs (001) substrate. The intended structure parameters were: (i) an active region comprising an 8-nm thick pseudomorphic $In_{0.15}Ga_{0.85}As$ single QW between two 10-nm thick GaAs layers; (ii) two graded $Al_xGa_{1-x}As$ layers with $0.1 < x < 0.4$, which sandwiched the active region. Regions 1 and 2 of the sample were intentionally undoped; (iii) a cladding comprising an *n*-$Al_{0.4}Ga_{0.6}As$ bottom layer and a *p*-$Al_{0.4}Ga_{0.6}As$ top layer (the samples were supplied by SLI, 15 Link Drive Binghamton, NY 13904).

5.2.1. QW parameters

The SPV spectrum for photon energies lower than 1.55 eV for light intensity 700 nW cm^2 is shown in Fig.

3. The spectrum has five peaks (again the overall SPV is negative), and is typical for QW structures spectrum. Each peak position has been evaluated by Lorentzian fitting and is marked by an arrow in the figure [47].

The sensitivity to quantum effects was studied by solving the Schrödinger equation while varying growth and structure parameters. Fig. 4 shows the calculated dependence of the 1HH-1E (a) and 2HH-2E (b) transition levels on growth/structure parameters around their intentional growth values. The latter are taken as the zero points of the x-axes and correspond to the intended growth values and an electric field of 41 kV cm^{-1}. The measured transition energy is presented as a full circle and the measurement error is also indicated. The Al mole fraction although graded was taken as a constant 10% since its variation showed no significant effect on the transition energy. This simplification may give rise to larger errors for higher order transitions. The dependence on the GaAs layer width (not shown) also proved to be very weak.

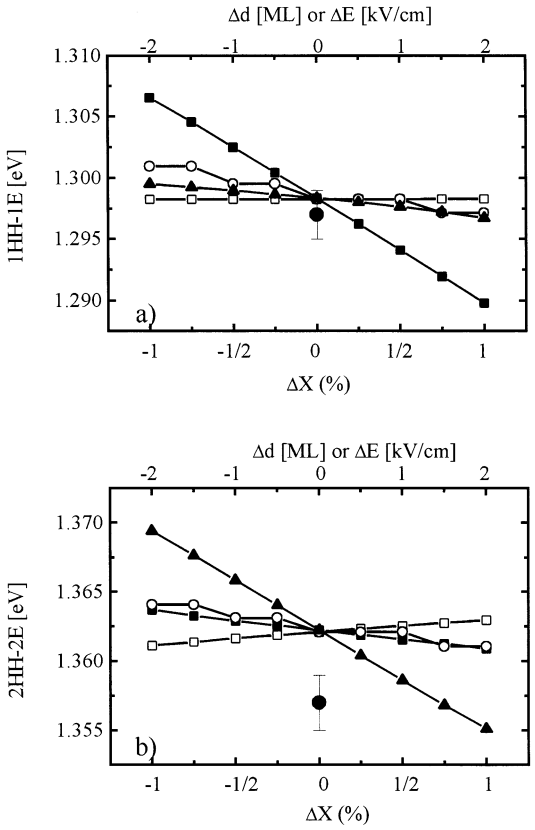

Fig. 4. Energies of (a) 1HH-1E and (b) 2HH-2E transitions as function of Al mole fraction (open squares, nominally $x = 10\%$), In mole fraction (full squares, nominally $x = 15\%$), InGaAs well width (open circles, nominally $d = 8$ nm) in monolayers (ML), and electric field (full triangles, nominally $E = 41$ kV cm^{-1}). The experimental energy value of each transition is denoted by a full circle.

Table 2
Experimental and calculated transition energies of the GRINSCH laser[a]

Transition	Experimental		Calculated	
	eV	nm	eV	nm
1HH-1E	1.297	956	1.297	956
1LH-2E/1HH-3E/1HH-4E	1.324	937	1.329/1.323/1.334	933/937/930
2HH-2E	1.357	914	1.357	914
3HH-3E	1.409	880	1.415	876
4HH-4E	1.477	840	1.476	840

[a] Calculated values were obtained taking into account 8 meV of exciton binding energy.

Fig. 4 shows that each of these transition energies is strongly dependent on a single parameter. The first transition is sensitive to the In mole fraction. This is reasonable since In mole fraction affects the well material bandgap (also through strain) and therefore the well depth. The second transition is sensitive to the electric field because of the QCSE. (There is no single dominant parameter affecting the third and fourth transitions.) Thus, a fitting procedure, which takes into account the transitions energy and probability was employed. The enhanced dependence on the electric field and the In mole fraction made it possible to achieve a good fitting by varying these parameters while keeping other parameters at their intentional values. The fitting results for the electron-heavy hole for the most probable are presented in Table 2 and compared to the experimental values. These results were obtained using a 14.8% In mole fraction and an electric field of 45 kV cm^{-1}. (This result was confirmed by modulation spectroscopy results [48]). The accuracy of the In mole fraction determination was found to be $\pm 0.25\%$ and ± 1 kV cm^{-1} for the electric field. Other parameters have a smaller impact on the transition energies and probabilities and thus on the overall device performance.

The SPV peaks, observed in this spectral regime, are proportional to the probability of the transition. Indeed, the four strongest calculated transitions are experimentally resolved in the SPV spectrum of Fig. 3. The presence of a non-negligible electric field gives rise to otherwise 'forbidden' transitions. These transitions shape the peak and contribute to the background as well as transitions from light hole levels. Note that the feature at 1.324 eV ($\#$ 2 in Fig. 3) may originate from the 1LH-2E transition as well as the 1HH-3E and 1HH-4E transitions.

The 1HH-1E transition measured by SPS, although very accurate, is not a direct measure of the lasing wavelength since the transition level is red shifted due to the QCSE. The low excitation intensity (~ 7 μW at most) does not reduce the electric field by the same amount as in the forward bias required for device operation. Using the fitting results, the behavior of the QCSE can be evaluated by its electric field dependence.

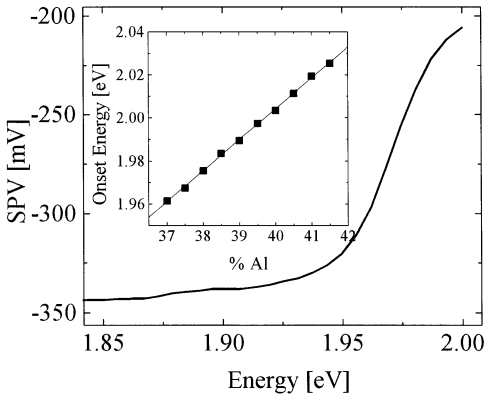

Fig. 5. The SPV spectrum for photon energies above 1.85 eV. The inset shows the dependence of the SPV onset energy on the cladding Al mole fraction.

From this behavior a lasing wavelength of ~ 951 nm (1.304 eV) is predicted.

5.2.2. The cladding layers

The high energy part of the spectrum is shown in Fig. 5. An onset in the SPV is observed at photon energy of ~ 1.96 eV. This part of the spectrum is governed by absorption in the highly doped $Al_{0.4}Ga_{0.6}As$ cladding layers. The absorption at the cladding evidently causes a slope change in the SPV, as shown in the figure. This may be caused by changes in the surface band banding and/or by light modulation due to absorption at this layer [17]. This sharp onset may be used for estimation of the cladding Al mole fraction. The inset of Fig. 5 shows the dependence of the onset energy on Al mole fraction extracted from simulations. The linear dependence is a manifestation of the linear dependence of the $Al_xGa_{1-x}As$ bandgap on x for $x < 0.45$ [49]. However, in order to accurately estimate the composition of the layer, other effects, such as sub-bandgap tails and bandgap narrowing, originating from the high doping, should be taken into account. Using the intentional doping, and a linear interpolation of the data for GaAs and AlAs [50], a value of 23 meV for the bandgap narrowing has been obtained. Adding it to the experimental bandgap, results in an estimated Al mole fraction of 39%, which is within 1% of the intentional value.

6. Conclusions

Surface photovoltage spectroscopy has been employed for studies of quantum well structures and devices at room temperature. The heavy hole to electron energy transition levels have been observed in the SPV spectra as well as signals from other regions of the structure. Numerical calculations have shown that the PV should increase with decreasing well width in single QW *p-i-n* structures. Effective carrier lifetimes at the well have been estimated, as well as well layer composition and width, and Al concentration at the highly doped cladding. Built-in electric fields at the active region have been estimated. Device parameters, such as lasing frequency, have also been evaluated. SPS emerges as a powerful tool for quantitative characterization of QW devices, and therefore can be used for quality control of QW structures and devices at initial stages of device formation in a contactless and non-destructive manner.

Acknowledgements

The authors are deeply indebted to Dr L. Kronik, Tel-Aviv University, Tel-Aviv, Israel; Professor K.W.J. Barnham, Dr J. Barnes, and Dr J. Nelson, Imperial College of Science, Technology and Medicine, London, UK; M.C. Hanna, National Renewable Energy Laboratory, Golden, CO, USA; and Professor F.H. Pollak, Brooklyn College of the City University of New York, New York, USA, for their cooperation in performing this research work, sharing their samples and data as well for their insight, interpretation and valuable discussions. Y.S. is grateful to Dr and Mrs Krongeld for their generosity.

References

[1] C. Weisbuch, B. Vinter, Quantum Semiconductor Structures, Academic Press, San Diego, 1991.
[2] J. Singh, Physics of Semiconductors and their Heterostructures, McGraw-Hill, New York, 1993.
[3] G. Bastard, Wave Mechanics Applied to Semiconductor Heterostructures, Les Editions de Physique, Les Ulis, 1988.
[4] F.H. Pollak, H. Shen, Mater. Sci. Eng. R10 (1993) 275.
[5] F.H. Pollak, W. Krystek, M. Leibovitch, M.L. Gray, W.S. Hobson, IEEE J. Selected Topics Quant. Elect. 1 (1995) 1002.
[6] W. Krystek, M. Leibovitch, F.H. Pollak, G. Gumbs, G.T. Barnham, X. Wang, J. Appl. Phys. 84 (1998) 2229.
[7] P. Blood, J. Appl. Phys. 58 (1985) 2288.
[8] X. He, M. Razeghi, Appl. Phys. Lett. 62 (1993) 618.
[9] S.Y. Wang, Y. Kawakami, J. Simpson, H. Stewart, K.A. Prior, B.C. Cavenett, Appl. Phys. Lett. 62 (1993) 1715.
[10] K. Kawasaki, M. Imazawa, K. Kawashima, K. Fujiwara, M. Hosoda, K. Tominaga, J. Appl. Phys. 84 (1998) 3338.
[11] K. Kawasaki, M. Imazawa, T. Imanishi, K. Kawashima, K. Fujiwara, M. Hosoda, K. Tominaga, Jpn. J. Appl. Phys. Part 1 38 (1999) 2552.
[12] K. Tanaka, N. Kotera, H. Nakamura, J. Appl. Phys. 85 (1999) 4071.
[13] W. Zhu, Q. Shen, S. Liu, J. Condens. Matter. 7 (1995) 9693.
[14] I.A. Karpovich, V.Ya. Aleshkin, A.V. Anshon, T.S. Babushkina, B.N. Zvonkov, S.M. Malkina, Fiz. Tekh. Poluprovodn. 24 (1990) 2172 [Sov. Phys. Semicond. 24 (1990) 1346].
[15] I.A. Karpovich, D.O. Filatov, Fiz. Tekh. Poluprovodn. 30 (1996) 1745 [Semiconductors 30 (1996) 913].

[16] J. Hlávka, K. Ploog, J. Appl. Phys. 70 (1991) 3362.
[17] L. Kronik, Y. Shapira, Surf. Sci. Rep. 37 (1999) 1.
[18] Lord Kelvin, Philos. Mag. 46 (1898) 82.
[19] J. Lagowski, Surf. Sci. 299/300 (1994) 92.
[20] L. Burstein, Y. Shapira, B.R. Bennett, J.A. delAlamo, J. Appl. Phys. 78 (1995) 7163.
[21] L. Kronik, M. Leibovitch, E. Fefer, V. Korobov, Y. Shapira, J. Elec. Mater. 24 (1995) 893.
[22] L. Kronik, L. Burstein, M. Leibovitch, Y. Shapira, D. Gal, E. Moons, J. Beier, G. Hodes, D. Cahen, D. Hariskos, R. Klenk, H.-W. Schock, Appl. Phys. Lett. 67 (1995) 1405.
[23] M. Leibovitch, L. Kronik, B. Mishori, Y. Shapira, C.M. Hanson, A.R. Clawson, P. Ram, Appl. Phys. Lett. 69 (1996) 2587.
[24] E. Moons, M. Eschle, M. Gratzel, Appl. Phys. Lett. 71 (1997) 3305.
[25] M. Eschle, E. Moons, M. Gratzel, Opt. Mater. 9 (1998) 138.
[26] B. Goldstein, D. Redfield, D.J. Szostak, L.A. Carr, Appl. Phys. Lett 39 (1981) 258.
[27] C. Munakata, N. Honma, Jpn. J. Appl. Phys. 26 (1981) L856.
[28] D.J. Szostak, B. Goldstein, J. Appl. Phys. 56 (1984) 522.
[29] L. Kronik, B. Mishori, E. Fefer, Y. Shapira, W. Riedl, Sol. Ener. Mater. Sol. Cells 51 (1998) 21.
[30] B. Mishori, M. Leibovitch, Y. Shapira, F.H. Pollak, D.C. Streit, M. Wojtowicz, Appl. Phys. Let. 73 (1998) 650.
[31] H. Akera, S. Wakahara, T. Ando, Surf. Sci. 196 (1988) 694.
[32] G.A. Ashkinazi, M.G. Leibovitch, M. Nathan, IEEE Trans. ED 40 (1993) 285.
[33] M. Leibovitch, Ph.D. Thesis, Tel-Aviv University (1994).
[34] S. Selberherr, Analysis and Simulation of Semiconductor Devices, Springer, New York, 1984.
[35] L. Burstein, J. Bregman, Y. Shapira, J. Appl. Phys. 69 (1991) 2312.
[36] S. Wang, Fundamentals of Semiconductor Theory and Device Physics, Prentice-Hall, Englewood Cliffs, NJ, 1989, p. 618.
[37] P. Blood, J. Appl. Phys. 58 (1985) 2288.
[38] J. Hlávka, K. Ploog, J. Appl. Phys. 70 (1991) 3362.
[39] N. Bachrach-Ashkenasy, L. Kronik, Y. Shapira, Y. Rosenwaks, M.C. Hanna, M. Leibovitch, P. Ram, Appl. Phys. Lett. 68 (1996) 879.
[40] S.M. Sze, Physics of Semiconductor Devices, second ed, New York, Wiley, 1981.
[41] J. Barnes, E.S. M. Tsui, K.W.J. Barnham, S.C. McFarlane, C. Button, J.S. Roberts, J. Appl. Phys. 81 (1997) 892.
[42] J. Nelson, in: M.H. Francombe, J.L. Vossen (Eds.), Physics of Thin Films, vol. 21, Academic Press, London, 1995, p. 311.
[43] G. Haarpaintner, J. Barnes, K. Barnham, J.P. Conolly, S.S. Dosanjh, J. Nelson, C. Roberts, C. Button, G. Hill, M.A. Pate, J.S. Roberts, Proceedings of the 1st World Conference on Photovoltaic Energy Conversion, Hawaii, 1994, p. 1783.
[44] R. Winkler, Phys. Rev. B51 (1995) 14395.
[45] L.C. Andreani, in: E. Burstein, C. Weisbuch (Eds.), Confined Electrons and Photons, Platinum Press, New York, 1995, p. 57.
[46] F.-Y. Juang, J. Singh, P.K. Bhattacharga, K. Bajema, R. Merlin, Appl. Phys. Lett. 48 (1986) 1246.
[47] N. Ashkenasy, M. Leibovitch, Y. Shapira, F.H. Pollak, T. Burnham, X. Wang, J. Appl. Phys. 83 (1998) 1146.
[48] W. Krystek, M. Leibovitch, F.H. Pollak, G. Gumbs, G.T. Barnham, X. Wang, J. Appl. Phys. 84 (1998) 2229.
[49] F.H. Pollak, in: S. Adachi (Ed.), Properties of Aluminum Gallium Arsenide, INSPEC, London, 1993, p. 53.
[50] L. Pavesi, M. Guzzi, J. Appl. Phys. 75 (1994) 4779.